Scandinavian Blocking Modulates Intense Rain Events in Svalbard

Francois Lapointe[1], Ambarish Karmalkar[2], Raymond Bradley[1], Michael Retelle[3,4]

[1]University of Massachusetts, Dpt of Earth, Geographic, and Climate Sciences. Amherst, MA. USA.
[2]University of Rhode Island, Dpt of Geosciences [3]Bates College, Dpt of Geology &[4]University Center in Svalbard.

NSF Award # 1744515

1 Background

Svalbard is located at the forefront of Arctic temperature amplification compared to other areas at similar latitudes due to the greater influence of the North Atlantic current. Arctic precipitation in the form of rain is forecast to become more prevalent in a warmer world. However, natural modes of variability may interfere to amplify or dampen this trend. Here, we show that rain and unusual warm events in Svalbard are intrinsically linked with periods of higher pressure over northern Scandinavia, i.e., Scandinavian Blocking. Rainfall episodes lead to coarse particle sedimentation in Linnévatnet, a lake in southwest Spitsbergen, with the coarsest sediments consistently deposited during these Scandinavian Blocking events. A unique annually resolved sediment record from Linnévatnet shows that this linkage has been persistent in the past. Precipitation trends have steadily increased since the mid-1850s, reaching unprecedented values in 2016. As warming continues and sea ice recedes, future Svalbard floods will become more intense during episodes of Scandinavian (& Ural) blocking.

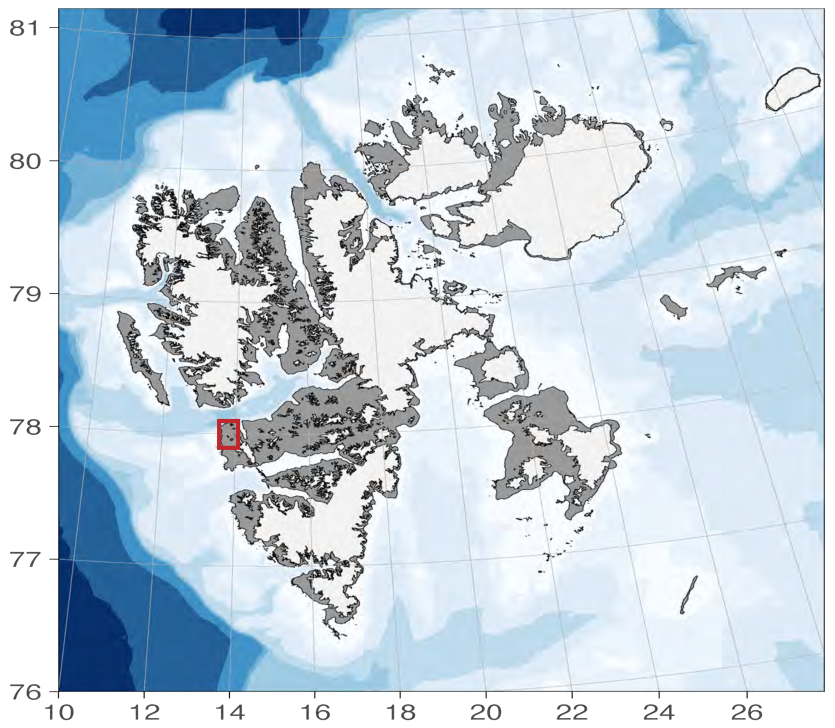

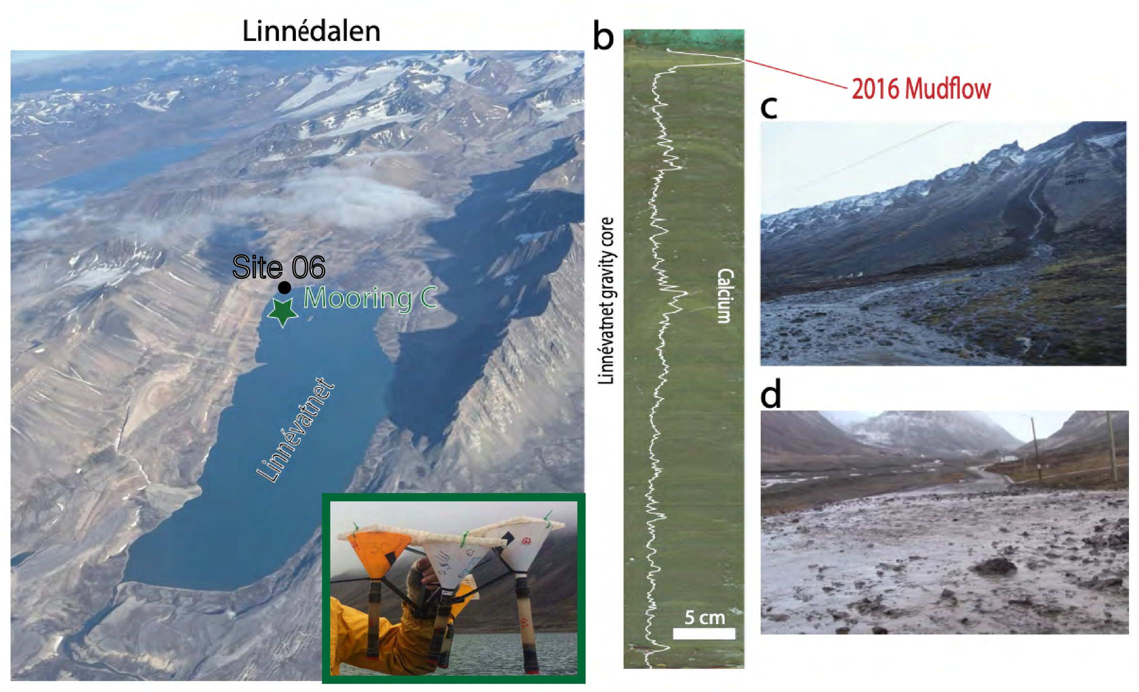

Sediment traps

Location of Linnevatnet Lake(red rectangle) in Svalbard. Mooring C is the location wheree the composite sediment sequence was collected as well as sediment traps. The 2016 mudflow was triggered by the largest rainfall event on record. The year 2016 is characterized by highest Ca values.

2 Varve chronology

Ct-scan varve mooring C

96 overlapping thin sections

Chemo-stratigraphy

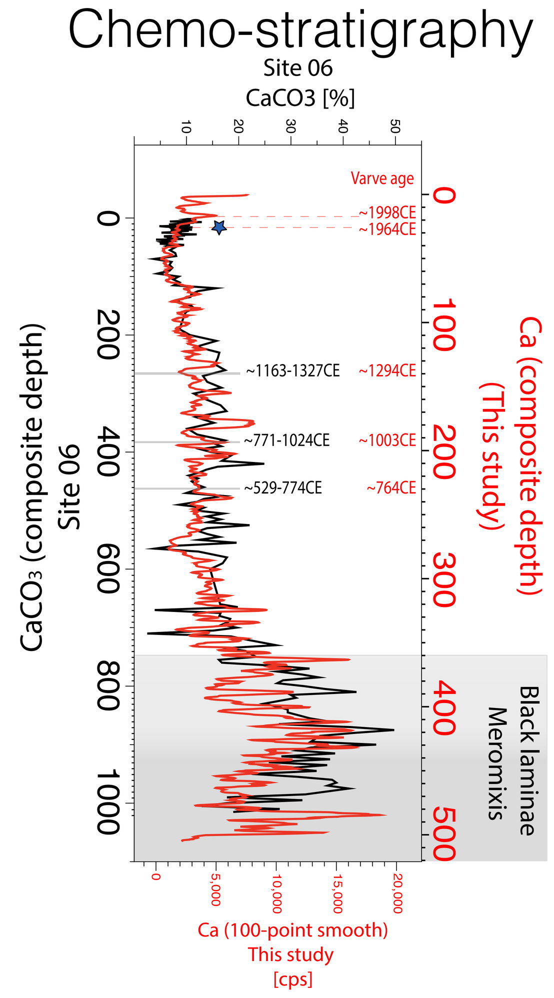

Age model

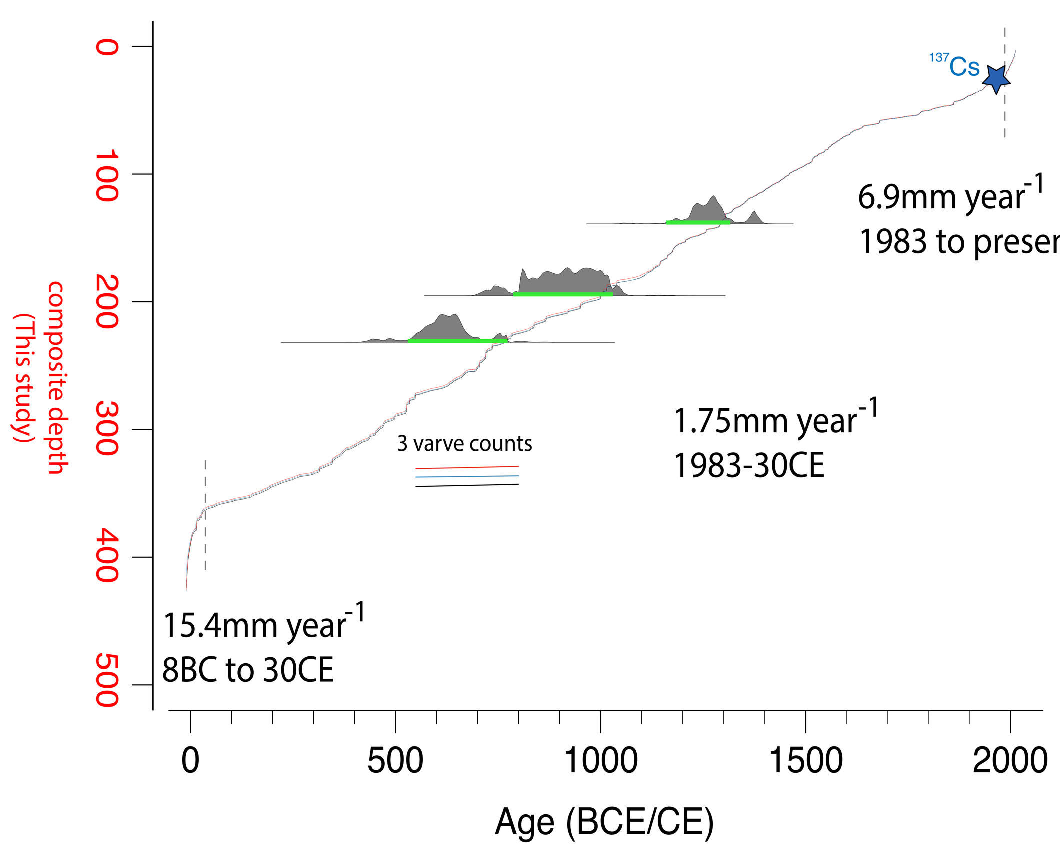

3 Sediment traps as witnesses of Blocking

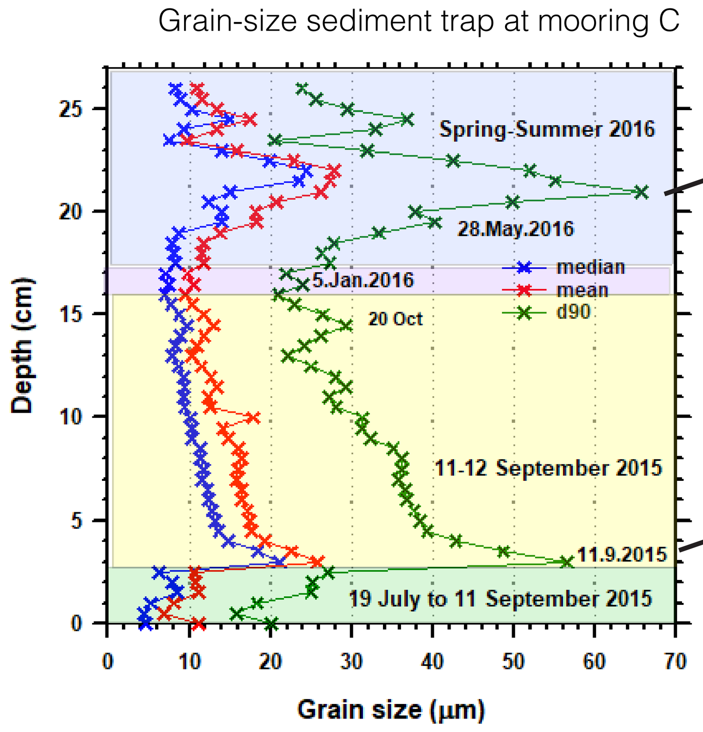

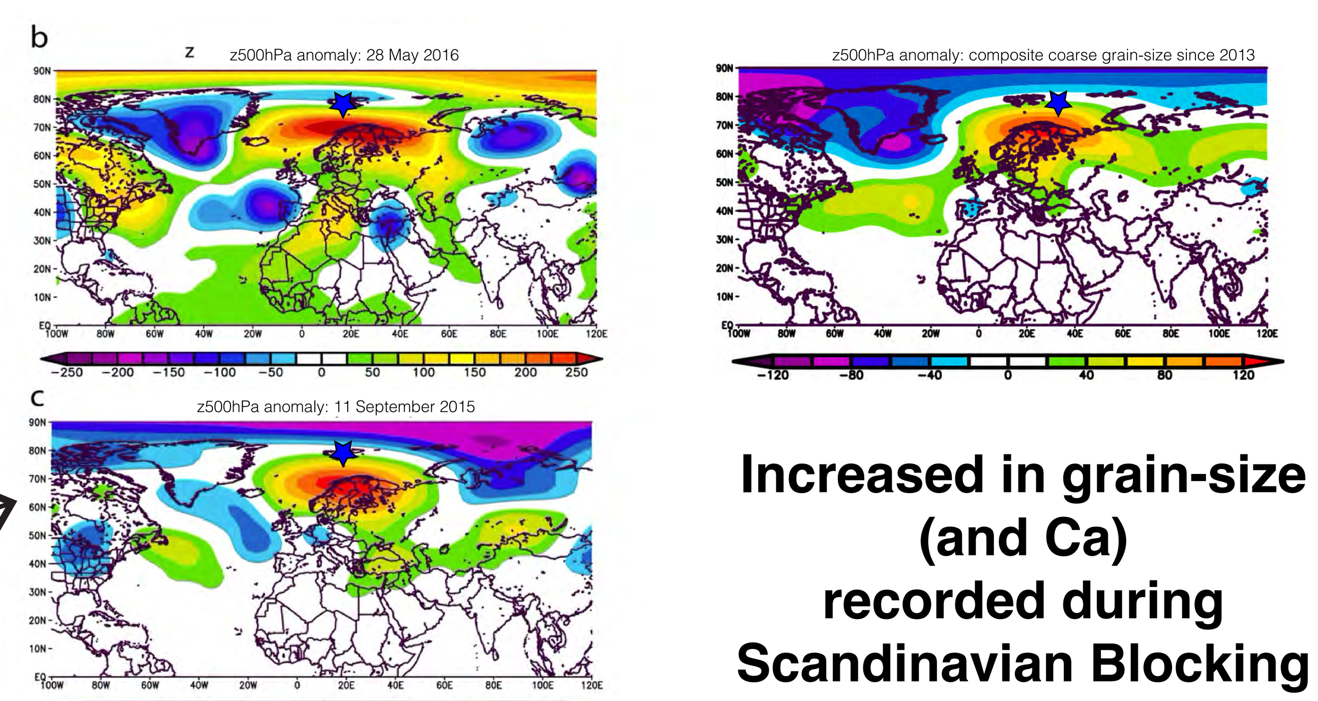

Increased in grain-size (and Ca) recorded during Scandinavian Blocking

a Grain-size data collected from the sediment trap at mooring C in 2015–2016 showing two days with coarsest grain-size peaking on September 11, 2015 and May 28, 2016, respectively. **b** and **c**, atmospheric pressure anomalies at 500 hPa Geopotential height (Z500) (relative to 1980–2010) during those two days calculated from daily National Centers for Environmental Prediction reanalysis data.

Sediment traps consist of a 12 cm diameter funnel carrying sediment to the receiving tube. The funnel is equipped with a baffle. The intervalometer recorded sedimentation at every 30 min at mooring C where the composite sediment core was retrieved.

4 Atmospheric blocking and Svalbard's precip

Monthly precip

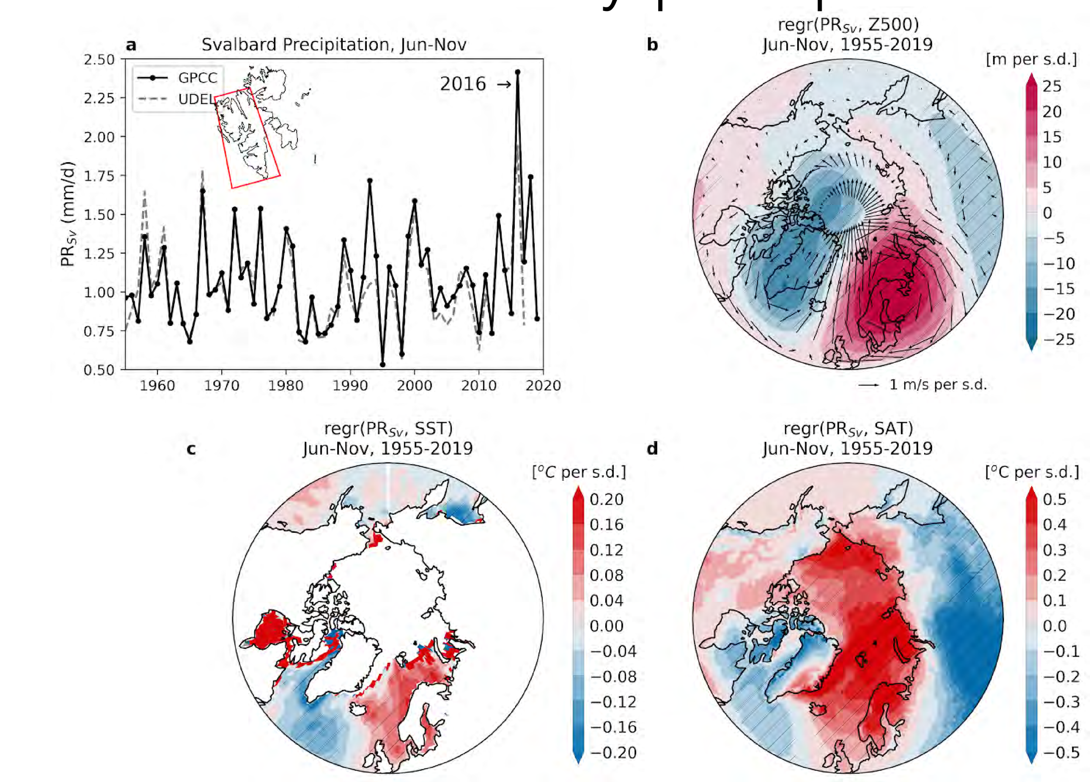

Past 2K

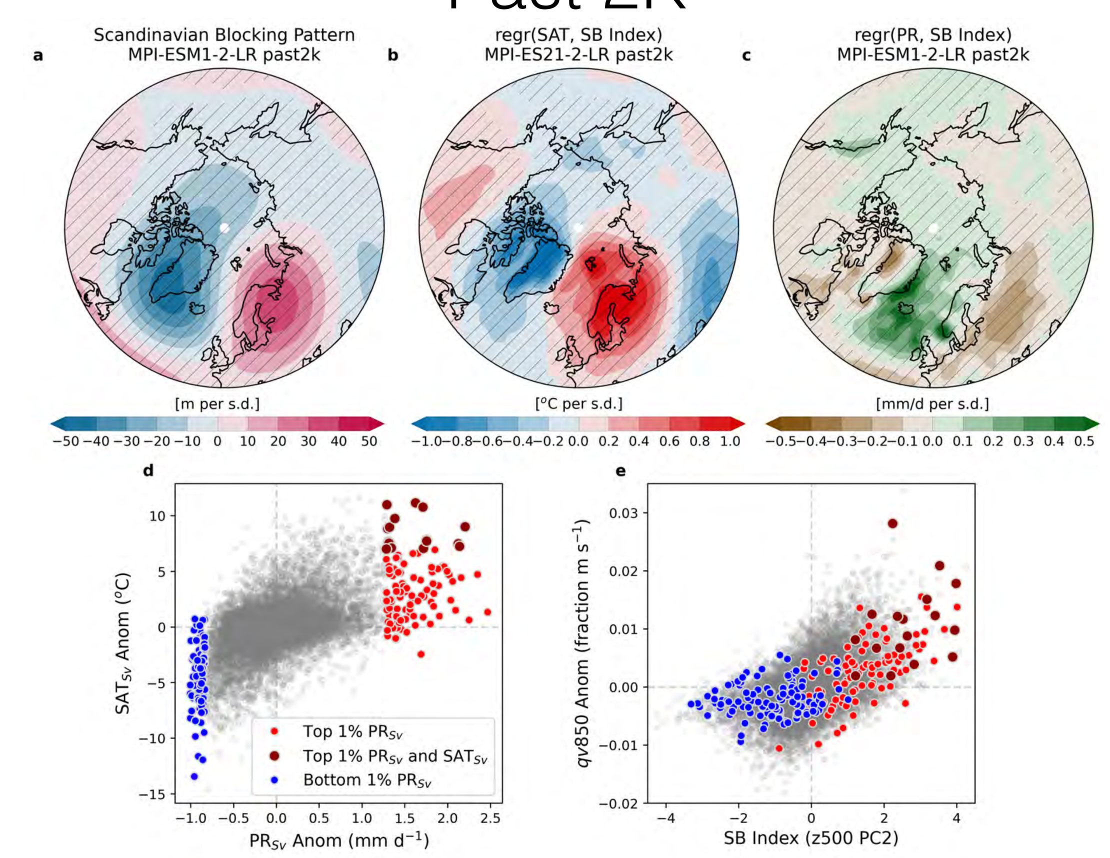

Left: Seasonal mean precipitation in Svalbard (PRSv; red rectangle in the inset) from June through November in two land-only observational datasets (see Methods): GPCC (solid black) and UDEL (dotted grey). **b**–**d**, Regression maps showing the relationship, for the period 1955-2019, between Jun-Nov monthly precipitation (GPCC PRSv) and (**b**) Z500 anomalies (colors) and winds (U500, V500; arrows) from ERA5; **c** SST anomalies from HadISST dataset and **d** surface air temperature (SAT) anomalies from ERA5. Regression maps show changes for one standard deviation change in the monthly PRSv time series. Cross-hatching shows regions with significant regression coefficients at the 95% significance level.
Right: **a**, Scandinavian Blocking pattern calculated by regressing Jun-Nov monthly Z500 anomaly field on the SB index. **b**,Regressions of Jun-Nov monthly temperature and the SB index. **c**, Regressions of Jun-Nov monthly precipitation and the SB index. **d**, Relationship between Jun-Nov monthly temperature and precipitation in over the period 1–1850 CE. The spatial average is calculated over the domain shown in left **a**. **e**, Relationship between the strength of the SB index and low-level moisture transport over the Greenland Sea.

5 Paleo evidence links SB to flood events

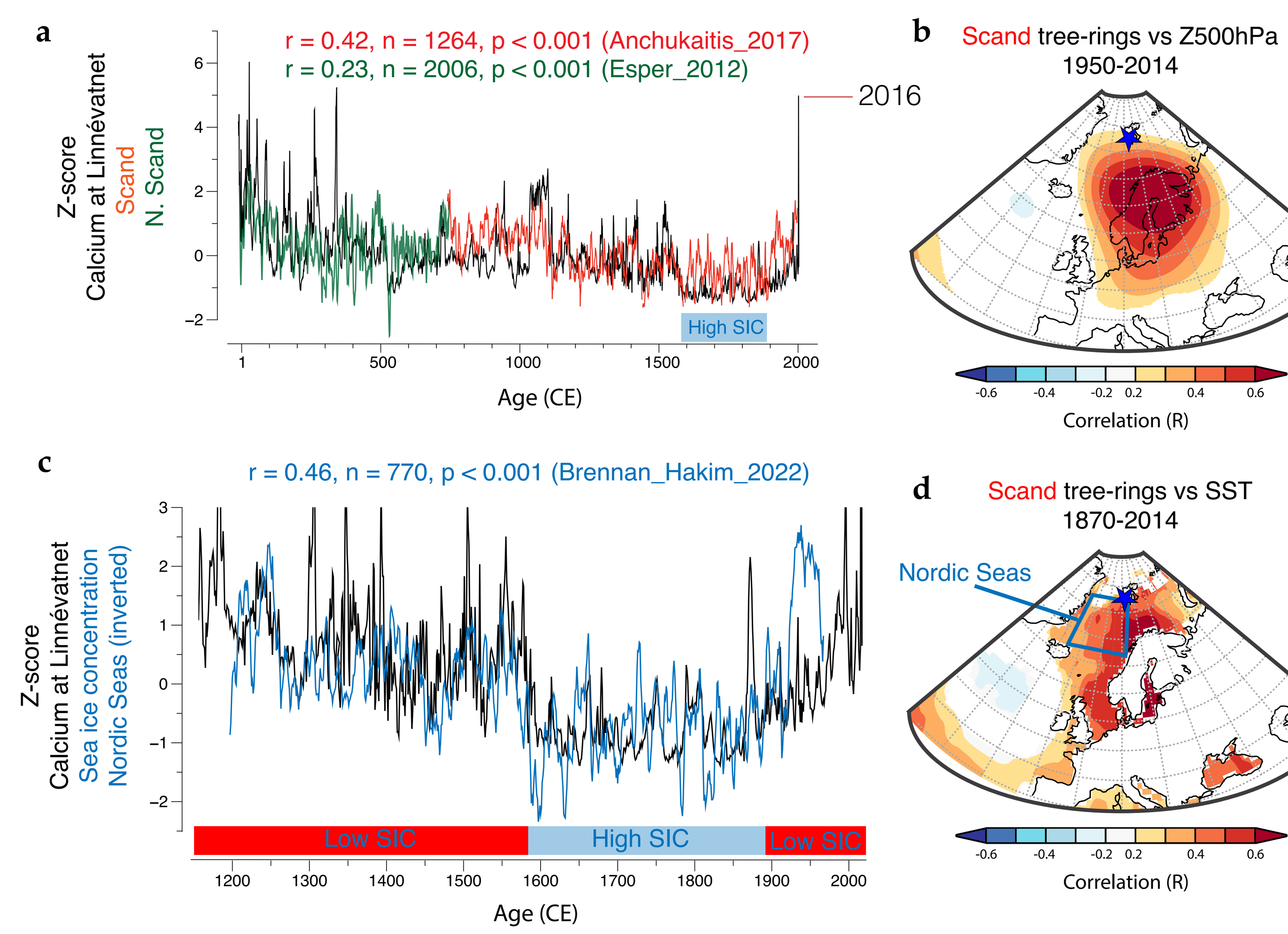

a, the Scandinavian (Scand) reconstructed summer temperatures from the N-TREND tree-ring dataset (in red; data were area-weight averaged over 12–30°E and 65–70°N) and the Northern Scandinavian reconstructed temperature (in green; N. Scand) from Esper et al. (2012) compared to the Calcium variability at Linnévatnet (in black). For visibility only the 1-750CE time interval is shown for the N. Scand (a; green) as the two Scand reconstructions exhibit strong co-variablity during their overlapping period (750 CE-2006 CE, annual: r = 0.87). **b**, Spatial correlation between the Scand temperature reconstruction (Anchukaitis et al. 2017) and atmospheric pressure at 500 hPa. The blue star denotes the location of Linnévatnet in Svalbard.

c, reconstructed sea ice concentration from the Nordic Seas (Brennan and Hakim 2022; blue) compared to the Calcium at Linnévatnet. Periods of lower and higher sea ice concentration (SIC) are highlighted in red and blue, respectively. **d**, Spatial correlation between the Scand temperature reconstruction and sea surface temperature from HadISST location of the targeted reconstructed SIC from the Nordic Seas in c. The tree-ring and sea-ice time series were filtered using 5-year running mean to improve visibility. Correlations shown (**b**,**d**) are significant with a P<0.1.

6 Future precip in Svalbard

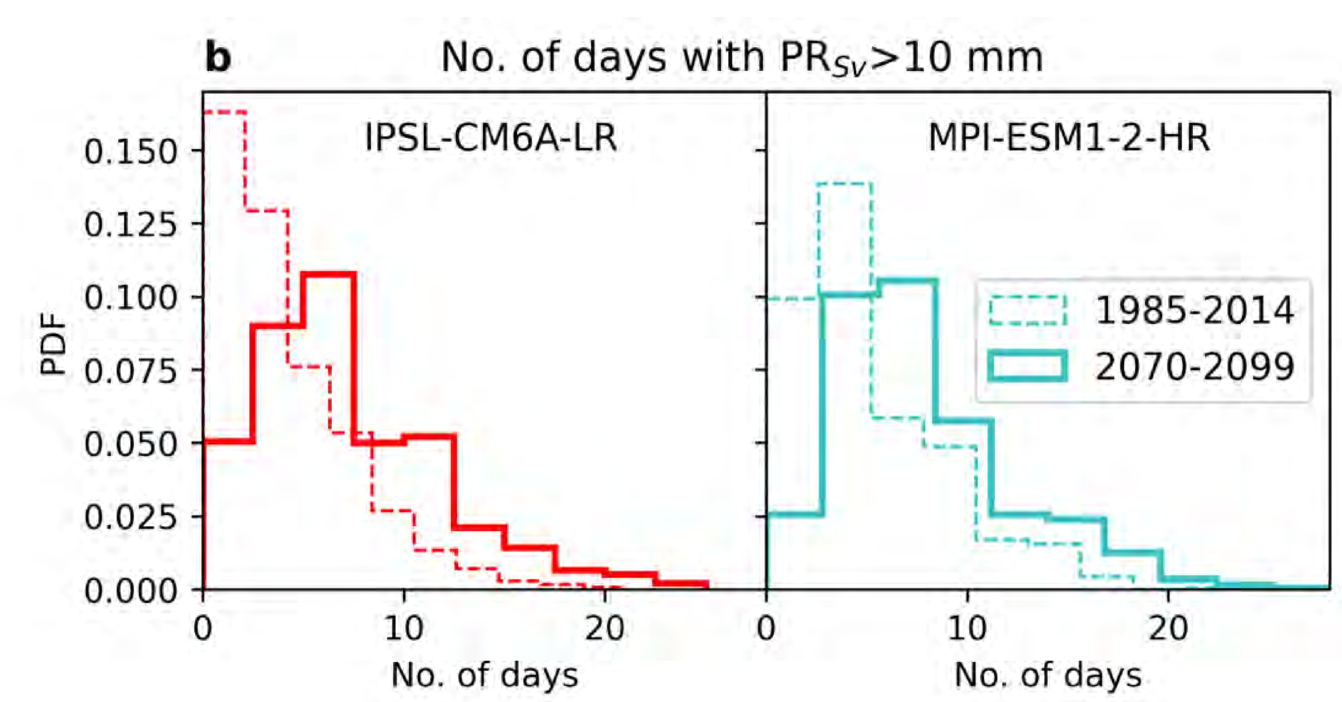

Histograms showing the distributions of number of days with precipitation > 10 mm across Svalbard (at 0.5° spatial resolution) over the period 1985-2014 (dashed line) and 2070-2099 (solid line) under SSP3-7.0 for IPSL-CM6A-LR (left) and MPI-ESM1-2-HR (right).

7 Conclusion

-Scandinavian and Ural blocking drive extreme precip in Svalbard. Linkage confirmed by observations, sediment traps and climate models

-Future precip on the rise with further warming. These rain events will be amplified during blocking events

8 References

Anchukaitis, K. J. et al. Last millennium Northern Hemisphere summer temperatures from tree rings: Part II, spatially resolved reconstructions. Quaternary Science Reviews 163, 1-22 (2017).
Brennan, M. K. & Hakim, G. J. Reconstructing Arctic sea ice over the Common Era using data assimilation. Journal of Climate 35, 1231-1247 (2022).
Esper, J. et al. Orbital forcing of tree-ring data. Nature Climate Change 2, 862-866 (2012).
Jungclaus, J. H. et al. simulating the common era: the Past2K working group of PmiP. Past Global Changes Magazine 29, 72-73 (2021)
Lapointe, F. et al. Multi-proxy evidence of unprecedented hydroclimatic change in a high Arctic proglacial lake: Linnévatnet, Svalbard. Arctic, Antarctic, and Alpine Research 55, 2223403 (2023).
Lee, S. H., Charlton-Perez, A. J., Furtado, J. C. & Woolnough, S. J. Representation of the Scandinavia–Greenland pattern and its relationship with the polar vortex in S2S forecast models. Quarterly Journal of the Royal Meteorological Society 146, 4083-4098 (2020).
Svendsen, J.I., Mangerud, J. Holocene glacial and climatic variations on Spitsbergen, Svalbard. The Holocene 7, 45-57 (1997)